www.sciencemag.org/cgi/content/full/312/5778/1375/DC1

Supporting Online Material for

Size Matters More Than Chemistry for Cloud-Nucleating Ability of Aerosol Particles

U. Dusek, G. P. Frank, L. Hildebrandt, J. Curtius, J. Schneider, S. Walter, D. Chand, F. Drewnick, S. Hings, D. Jung, S. Borrmann, M. O. Andreae

Published 2 June 2006, *Science* **312**, 1375 (2006)
DOI: 10.1126/science.1125261

This PDF file includes:

Materials and Methods

The CCN counter system

The system for measuring size-resolved CCN spectra consists of a differential mobility analyzer (DMA; a TSI 3071 Electrostatic Classifier, changed to closed-loop arrangement) followed by a CCN counter (static thermal diffusion chamber) (*S1*), and condensation particle counter (CPC; TSI 3762) measuring in parallel. Ambient particles were sampled from a whole air inlet approximately 10 m above ground level and dried in a diffusion drier to relative humidities below 35%. Losses in the dryer were insignificant for particle sizes above 15 nm. Subsequently, charge equilibrium was imposed on the particles in a bipolar charger (^{63}Ni) and the DMA was used to select a fraction of particles within a narrow mobility range. The DMA was applied with a relatively wide transfer function (aerosol to sheath flow ratio 1:3) and a sheath flow humidity of less than 10%. The number concentration of particles exiting the DMA (CN) was measured by the CPC, whereas the CCN counter counted only the particles that were activated to cloud droplets at a certain supersaturation (S). The fraction of activated particles at each DMA size setting and each S could be directly calculated as CCN/CN.

A DMA generally selects particles with equal electrical mobility, which can be uniquely converted to mobility equivalent particle diameter (d_p), if the number of charges on the particle is known. Each selected mobility fraction contains not only particles with a single charge and desired particle diameter d_p, however, but also a small fraction of particles with multiple charges and correspondingly larger particle diameters. These particles are activated at a lower S than the smaller, singly charged particles and thus lead to artificially high CCN efficiencies. We therefore correct for the presence of these particles.

The static thermal-gradient diffusion chamber uses a laser to illuminate and a CCD camera to count droplets formed by the activated CCN at each S. The CCN counter was calibrated in the laboratory prior to the field experiment with respect to supersaturation and number concentration as described in (*S1*). The detection efficiency of the CCN counter is approximately 50 droplets cm^{-3}, which corresponds to 3 droplets in the sensing volume.

A typical CCN spectrum is recorded by selecting a particle size fraction in the DMA and measuring CCN/CN ratios at increasing S until all particles are activated. In the FACE-2004 experiment we used 5 different particle diameters (40, 60, 80, 100, and 120 nm) and for each diameter 5 different supersaturations ranging from 0.25 to 2%. Since the time required for one CCN measurement is almost 1 minute, one full scan of all diameters and supersaturations takes approximately 20 minutes. The particle concentrations exiting the DMA are generally lower than 100 cm^{-3} and thus close to or even below the detection level of the CCN counter. We therefore averaged 6 hours of CCN measurements (approximately 16 spectra) to reduce the random variation by a factor of 4. The averaging was applied to the raw data and the number calibration and correction for doubly charged particles were applied to the averaged CCN spectra. This was necessary to avoid correcting into the data set the random noise, which for a single spectrum was of the order of the signal.

The AMS chemical measurements:

The Aerodyne Aerosol Mass Spectrometer (AMS) as well as its data evaluation have been described elsewhere (*S2*-*S4*). It is capable of determining size resolved mass concentrations of the submicron non-refractory aerosol with a high time resolution. In the analysis presented here, we used the size resolved mass concentrations of the 4 non-refractory species sulfate, nitrate, ammonium and total organics, with emphasis on the ratio of inorganic to organic aerosol compounds. The averaged total size distributions for the 4 case studies given in Table 1 are shown in Figure *S1*.

The diameter measured by the AMS is the so-called "vacuum-aerodynamic diameter", d_{va} (*S5*), which for spherical particles is related to the geometric diameter d_g by:

$$d_{va} = \frac{\rho_p}{\rho_0} d_g \qquad (1)$$

where ρ_p is the particle density in g cm^{-3}, and ρ_0 is the unit density (1 g cm^{-3}). By combination of different sizing techniques it is therefore possible to obtain the particle density. Here we used the diameter measured by a scanning mobility particle sizer (SMPS), which for spherical particles equals the geometric diameter. The ratio of the modal diameters of the measured size distributions gives the average particle density, which was 1.6 g cm^{-3} averaged over the whole measurement period. The averaged mass loadings were calculated for vacuum aerodynamic diameters below 208 nm, corresponding to a geometric diameter of 130 nm.

Detailed description of the case studies:

Figure S2 shows a map of the Kleiner Feldberg area and the surrounding cities, which are possible sources of recent pollution. The greater area of Frankfurt lies to the southeast of the field site and the cities Mainz and Wiesbaden lie to the southwest. During time periods with southeasterly and southwesterly wind direction aged urban pollution was advected to the field site. According to the Local Model (LM) of the German weather service (Deutscher Wetterdienst, DWD) typical transport times from Frankfurt to the Kleiner Feldberg site varied between 2 and 4 hours.

4-day air mass back trajectories were calculated every six hours with the NOAA HYSPLIT model. The back trajectories for the 4 selected case studies are shown in Figure S3A-D. Some major cities in or near the heavily industrialized Ruhr region (Köln, Düsseldorf, and Dortmund) are indicated by blue diamonds. In the case CONT1 (Figure S3A) the air masses circled over the Ruhr region which shows high SO_2 emissions in the EMEP emission inventory (*S6*). In the case MAR (Figure S3B) the air masses traveled over land for less than one day and stayed just to the north of the Ruhr region. In the CONT2 air mass case (Figure S3C) the air mass back trajectories did not cross any major industrial areas. Local trajectories and wind directions indicate that in these three cases, the last hours before reaching the field site were spent over the rural wooded areas to the north of the field site. In the case POLL (Figure S3D) the air masses originate in the north, but during the 24-hour measurement time period local wind directions are consistently from the southeast, indicating that local pollution from Frankfurt was advected to the field site.

Sensitivity studies:

Figure S4A - D gives an overview of the results of the first sensitivity study. Total CCN concentrations at S = 0.25% and 1%, were obtained by integrating CCN size distributions (see examples in Figure 2) for each 6-hour time interval. To obtain actual CCN concentrations (base case) at a given S, CCN size distributions were calculated using 6-hour average size distributions and corresponding CCN efficiencies. Total CCN concentrations (CCN_{tot}) at supersaturation S can be expressed as:

$$CCN_{tot}(S) = \sum_{d_i = d_{min}}^{d_{max}} \frac{dN}{d\log(d_i)} \cdot \frac{CCN}{CN}(S, d_i) \cdot \Delta\log(d_p), \quad (2)$$

where $dN/d\log(d_i)$ is the 6-hour average of the size distribution at diameter d_i, $\Delta\log(d_p)$ stands for the logarithm of the SMPS size interval, and $CCN/CN(S,d_i)$ the 6-hour average of the CCN efficiency, linearly interpolated to diameter d_i and S. For the sensitivity study case A (assuming constant CCN efficiencies) the 6-hour average CCN/CN ratios in Equation (2) are replaced by the average ratio over the whole field campaign. For case B (assuming constant size distributions) the 6-hour averaged $dN/d\log(d_i)$ are replaced by the average size distribution.

Figures S4A and C show scatter plots of the correlation between actual CCN_{tot} and modeled CCN_{tot} assuming constant aerosol composition (represented by constant mean CCN efficiencies, case A). In general, the actual CCN_{tot} can be modeled very well with these assumptions. As the supersaturation increases, the coefficient of determination increases, indicating that chemical effects become less important. At S = 0.25% 4 data points at high CCN concentrations clearly lie below the 1:1 line. These 4 data points correspond to the case CONT1 described in the previous section, where the aerosol particles are very efficiently activated due to a high inorganic ion content. However, at S = 1% even this relatively strong effect of particle chemical composition does not influence CCN_{tot} significantly. Panels B and D on the right side of Figure S4 show the correlation between actual CCN_{tot} and modeled CCN_{tot}, assuming a constant mean size distribution for the entire field campaign, but varying composition (CCN efficiencies). It is clear that total CCN concentrations cannot be modeled well based on knowledge of the CCN efficiencies or detailed chemistry alone.

Figure S5 shows similar correlation plots for total CCN concentrations normalized by the concentration of particles larger than 10 nm (CN10). In this case, the strong influence of total particle concentrations on CCN_{tot} is eliminated and only the shape of the (normalized) size distribution is important. Therefore, the dependence of CCN_{tot}/CN10 on the size distribution is weaker and the particle chemical composition is more important, especially at low S. For example, Figures S5A and C show that by using constant CCN efficiencies, high CCN_{tot}/CN10 ratios are consistently underestimated. The highest CCN_{tot}/CN10 ratios are only found for both large mean diameters of the size distribution combined with low cut-off diameters (high CCN efficiency). Overall, however, a time dependent size distribution combined with average CCN efficiencies is sufficient to approximate the CCN_{tot}/CN10 ratios with reasonable accuracy.

References:

(S1) G. P. Frank, U. Dusek, M. O. Andreae, in preparation.

(S2) J. T. Jayne, *et al., Aerosol Sci. Technol.* **33**, 49, (2000).

(S3) J. D. Allan, *et al., J. Geophys. Res.* **108**, 4090, doi:10.1029/2002JD002358, (2003)

(S4) J. L., Jimenez, *et al., J. Geophys. Res.* **108**, 8425, doi:10.1029/2001JD001213, (2003).

(S5) J. L. Jimenez, *et al., J. Geophys. Res.,* **108** 4318, doi:10.1029/2002JD002452, (2003).

(S6) UNECE, Present state of emission data, EB.AIR/GE.1/2003/10 (2003).

Figures

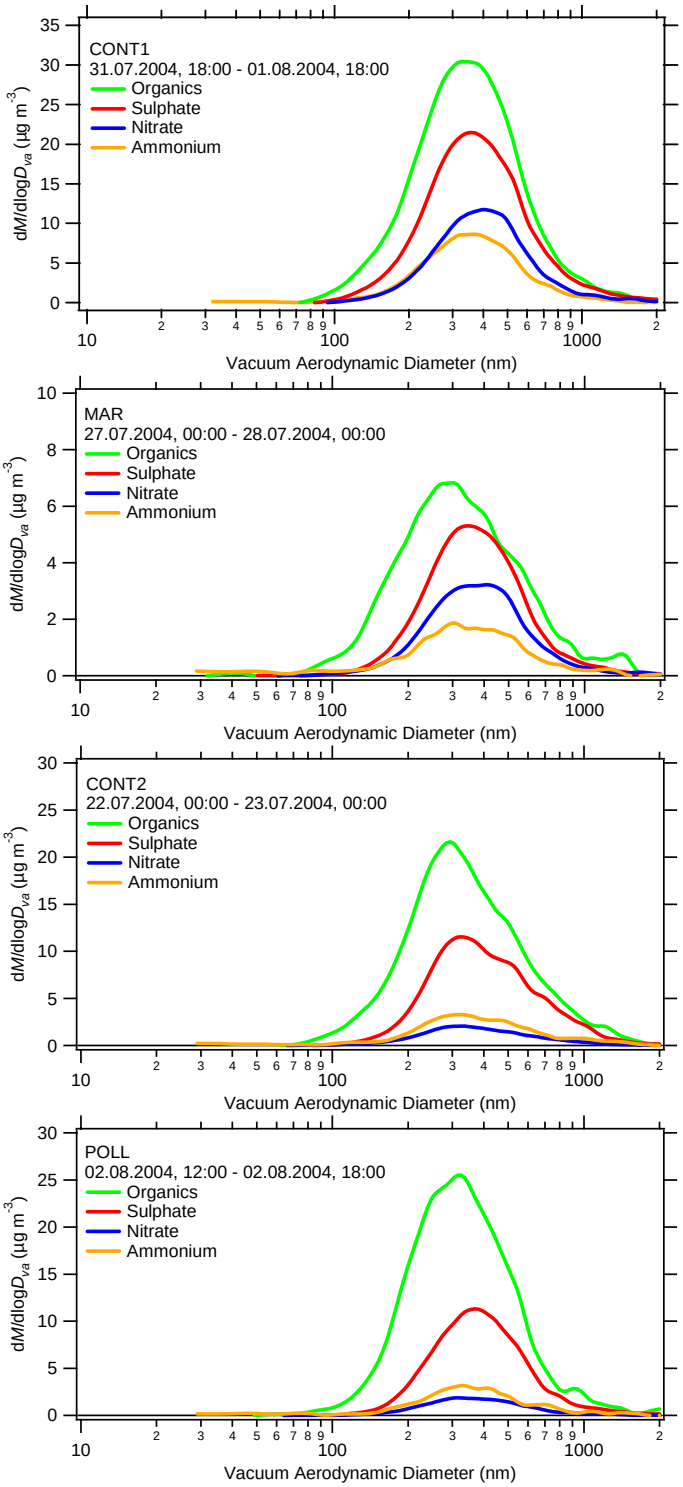

Figure S1. Chemically resolved size distribution recorded with the AMS for the 4 case studies given in Table 1.

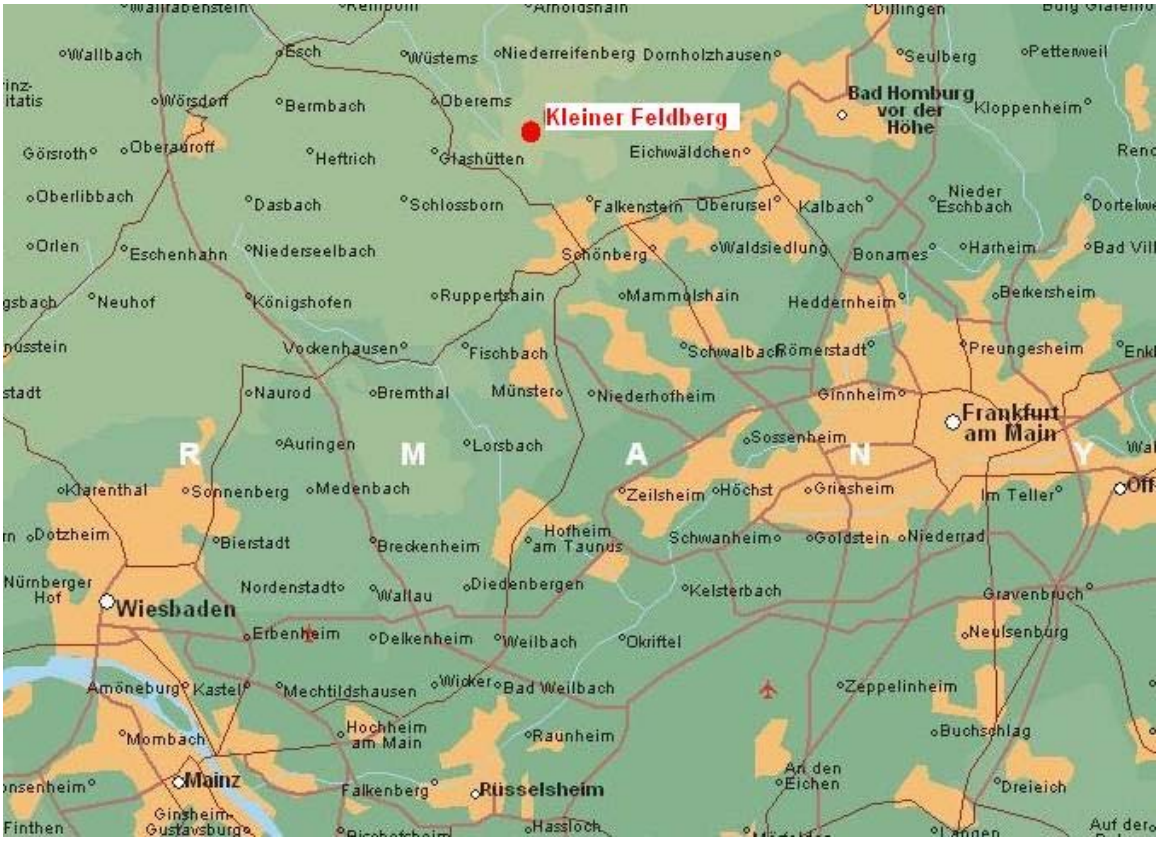

Figure S2. The 'Kleiner Feldberg' field site and surroundings

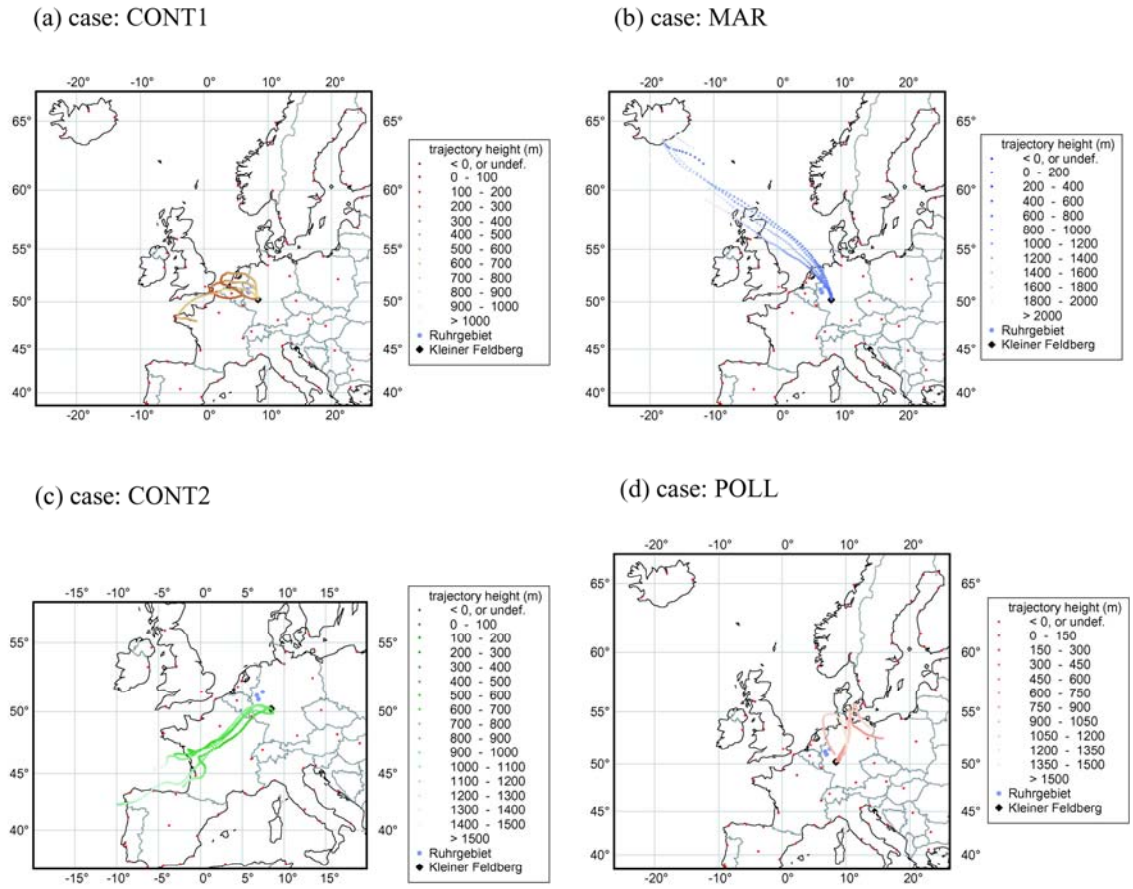

Figure S3: 6-day air mass back trajectories for the selected case studies

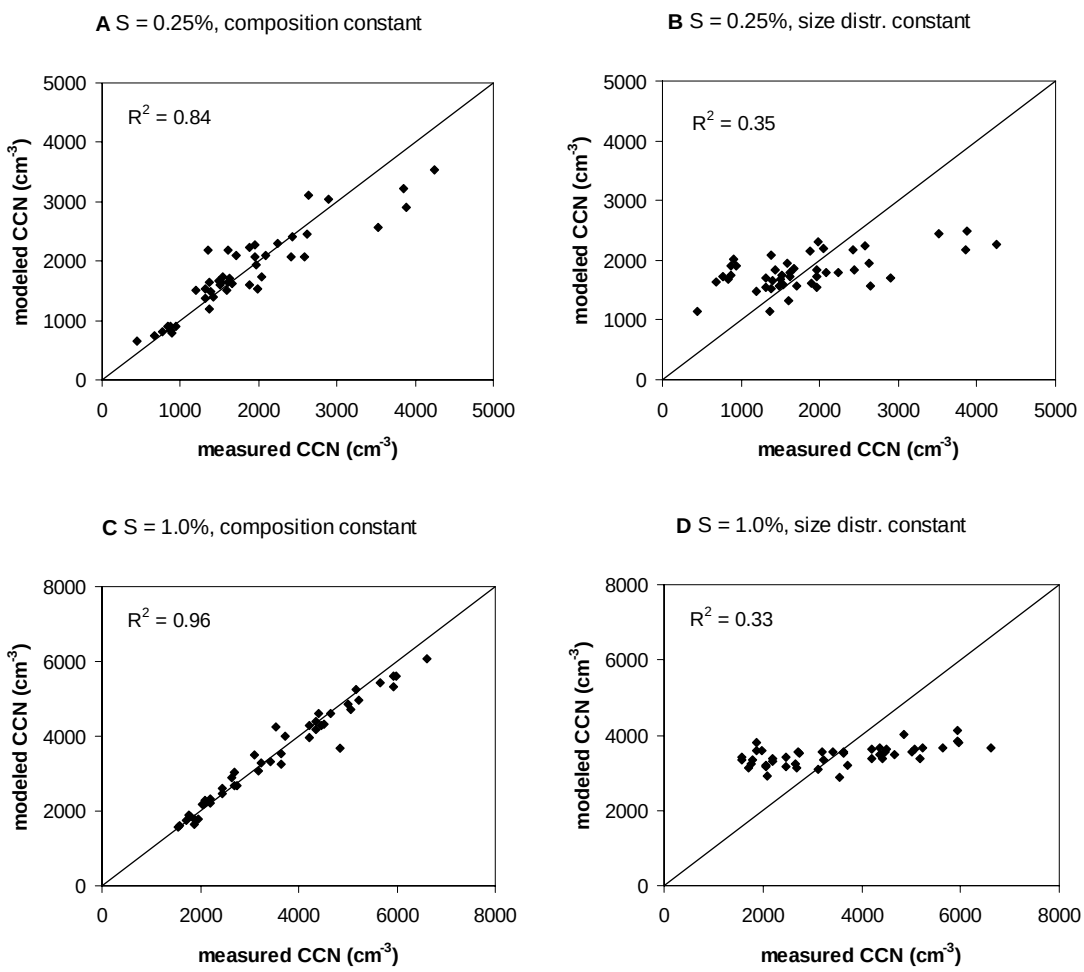

Figure S4. Correlation of actual CCN concentrations time series with simplified time series derived assuming constant composition (represented by mean constant CCN efficiencies) (panels A, C) and constant mean size distributions (panels B, D).

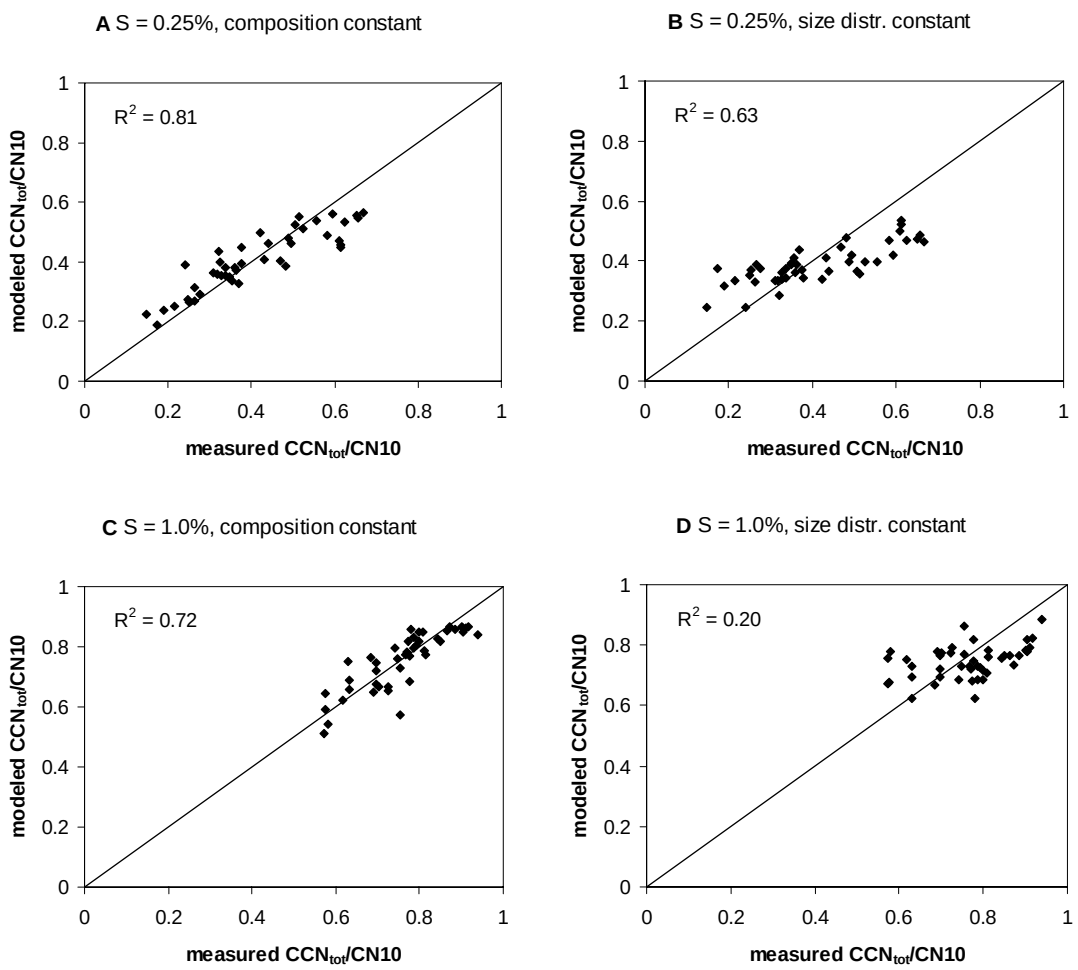

Figure S5. Correlation of time series of actual CCN/CN10 ratios with simplified time series derived using constant CCN efficiencies (panels A, C) and constant mean size distributions (panels B, D).